Investigation of Slotted ALOHA Under Nakagami Fading With Synchronized and Asynchronous Cochannel Cells

Lei Zhou, *Student Member, IEEE*, Yu-Dong Yao, *Senior Member, IEEE*, Harry Heffes, *Fellow, IEEE*, and Ruifeng Zhang, *Member, IEEE*

***Abstract*—The throughput performance of slotted ALOHA (S-ALOHA) in a cellular system and Nakagami fading environment is studied. Based on the signal capture model, the effects of the multiple access interference (MAI) from in-cell users and the cochannel interference (CCI) from cochannel cells are quantified analytically. Especially considered are the cases when asynchronism of cochannel cells is present, for which an approximation of the interference distribution is successfully applied to get a highly precise expression of the system throughput. Our study shows that though the MAI level and capture effect determine the basic behavior of the S-ALOHA, CCI significantly reduces the throughput of S-ALOHA and asynchronous CCI introduces an especially severe impairment. Our analytical framework is also able to incorporate additional channel conditions and system parameters like lognormal shadowing and the cellular cluster size.**

***Index Terms*—Cellular system, cochannel interference, Nakagami fading, slotted ALOHA.**

I. Introduction

SLOTTED ALOHA (S-ALOHA) [1] is widely used in wireless data networks as a multiple access scheme. Its maximum throughput is $1/e$, which is obtained using a collision model assuming noiseless channels and equal-power packets [2]. However, in cellular wireless networks, signal fading and cochannel interference, in addition to thermal noise, should be taken into account in network performance evaluation. Fading channels cause random variations in the received signal power from different users. This may reduce the successful rate of packet transmissions when there is no collision in the channel, but also make it possible that one of several independently faded competing data packets supersedes others in power and "captures" the receiver, which leads to an increase of system throughput [3], [4]. Therefore, a capture model addressing signal-to-interference-and-noise ratio (SINR) is more appropriate than the collision model for S-ALOHA system performance analyzes [5]–[7]. Note that both in-cell interference and cochannel interference need to be considered in characterizing the capture model.

Manuscript received October 19, 2002; revised July 2, 2003. The work of R. Zhang was supported in part by the ONR (N00014-03-1-0123).

L. Zhou, Y.-D. Yao, and H. Heffes are with the Department of Electrical and Computer Engineering, Stevens Institute of Technology, Hoboken, NJ 07030 USA.

R. Zhang is with the Department of Electrical and Computer Engineering, Drexel University, Philadelphia, PA 19104 USA.

Digital Object Identifier 10.1109/TVT.2003.819622

The performance of S-ALOHA with capture has been extensively studied in the past. Most of the work has assumed Rayleigh fading channels [8]–[17]. Some additionally addressed the impact of lognormal shadowing, near-far effects, modulation, error control codes, and/or diversity combining [10], [12], [13], [15]–[18]. The Rician fading channel model has also been studied [14], [19]. The Nakagami distribution [20], as a more general model for fading channels, has been used in some recent studies in evaluating S-ALOHA [14], [19], [21]–[24]. In those studies, the same Nakagami fading model (but may have different parameters) has been applied to both the desired user packet and interfering ones. Mixed fading models appeared in [14] and [19], i.e., Rician/Rayleigh and Rician/Nakagami, where the desired signal is subject to Rician fading and the interference signal is subject to Rayleigh (Nakagami) fading.

In the aforementioned studies, in-cell multiple access interference (MAI) and cochannel interference (CCI) are not distinguished. MAI is from the contending mobile users in the same cell as the desired signal; while CCI is from the mobile users in the cochannel cells operating with the same group of frequencies. Besides the different fading they may experience, they exhibit different traffic profiles because of, very possibly, asynchronism among different cells in terms of time slot boundaries which could be due to synchronization errors or the network architecture by design. The latter affects the distribution of the amount of interference to the desired data packet within a time slot, and consequently affects the capture probability and the system throughput. Though modeling multiple interferers with different fading parameters [25]–[27] can somewhat address the fading difference between MAI and CCI, it does not taken the traffic profile into account and thus is not readily applicable for throughput analysis.

Our work in this paper emphasizes the difference of MAI and CCI in analyzing the throughput of S-ALOHA with capture. MAI and CCI, as well as the desired packets, are all modeled as Nakagami faded signals, but with different fading parameters. We especially study how asynchronism of CCI affects the interference traffic profile (even under the same given traffic load) that in turn affects the capture probability and system throughput. The third contribution of this work is that we relate the different fading parameters of MAI and CCI to the cell radius and cochannel cell distance so that throughput-optimized frequency reuse distance is obtained.

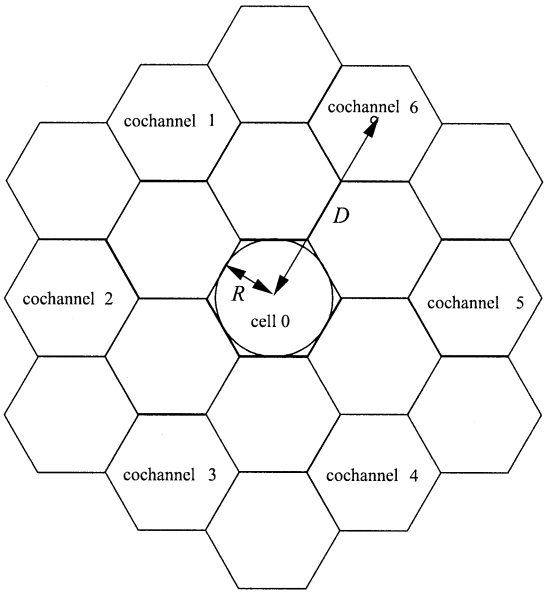

Fig. 1. In-cell interference (MAI) and cochannel cell interference (CCI) in a cellular system (an example of cluster size 7).

The rest of this paper is organized as follows. Section II presents the system model of S-ALOHA wireless packet access that we are to study, including the signal models for MAI and synchronized and asynchronous CCI and the Nakagami fading channel model. In Section III we derive the capture probability for given amount of MAI and CCI. The distribution of the number of MAI and CCI packets under both synchronous and asynchronous conditions is studied in Section IV. Section V discusses the relationship of the frequency reuse pattern and the system throughput. Some numerical and simulation results are given in Section VI. Finally, in Section VII, conclusions are drawn.

II. System Description

A. System Model

We consider a cellular packet radio system (see Fig. 1), in which data packets are transmitted from one mobile to another via a base station and the uplink communication (from mobiles to the base station) is through an S-ALOHA channel. We are interested in the throughput of this uplink channel. To this end, we adopt the model of infinite user population and Poisson data traffic [2], and we consider the capture effect caused by channel fading [10]. Denote with G the arrival rate in number of packets per cell per channel slot and with $P_{\rm cap}$ the probability that a test packet is captured by the base station receiver. Then the throughput of the uplink channel can be written as

$$S = GP_{\rm cap}. \tag{1}$$

The capture probability $P_{\rm cap}$ depends on the relative power level of the test packet and the interference.

The packet transmission in the uplink channel in one cell is subject to, in addition to additive noise and channel fading, two types of interference: MAI which is from contending transmissions in that cell, and CCI which is from transmissions in cochannel cells, as are shown in Fig. 1. Usually, the receiver decision variable for the tth symbol $s(t)$ of the test packet in the presence of $\mathrm{I}(t)$ MAI packets and $\mathrm{J}(t)$ CCI packets within the tth symbol duration is

$$r(t) = \sqrt{\mathrm{x}(t)}s(t) + \sum_{i=1}^{\mathrm{I}(t)} \sqrt{\mathrm{y}_i(t)}m_i(t) + \sum_{i=1}^{\mathrm{J}(t)} \sqrt{\mathrm{z}_i(t)}c_i(t) + w(t), \quad 1 \le t \le L \tag{2}$$

where $\mathrm{x}(t)$ is the received power of the tth symbol of the test packet, $\mathrm{y}_i(t)$ and $\mathrm{z}_i(t)$ are the received power of $m_i(t)$ and $c_i(t)$ which are the interfering symbols of the ith MAI packet and CCI packet, respectively, and $w(t)$ is the additive noise. $\mathrm{x}(t)$, $\mathrm{y}_i(t)$s and $\mathrm{z}_i(t)$s are random variables with distributions determined by the channel fading characteristics, and $\mathrm{I}(t)$ and $\mathrm{J}(t)$ are random variables with distributions determined by the data traffic. If the channel is slowly faded compared to the packet length L (which we assume in our following analysis), $\mathrm{x}(t)$ is constant across the test packet and thus the index t can be dropped. It is also feasible to assume that the MAI packets are all synchronized with the test packet; hence, $\mathrm{y}_i(t)$ and $\mathrm{I}(t)$ are also constant across the test packet and their index t can be dropped. The complication comes from the CCI. Depending on the synchronization mechanism of the cellular system, the effect of CCI can be different.

1) Synchronized Cochannel Cells: If a system-wide synchronization is achieved, the CCI from each cochannel cell, like the MAI, is synchronized with the test packet. Fig. 2(a) illustrates the perfect alignment of the transmission interval of the CCI packets from the 6 first-tier cochannel cells with the test packet. We can see that in the synchronization case, $\mathrm{z}_i(t)$ and $\mathrm{J}(t)$ are constant across the test packet and their index t can be dropped. In summary, the signal model of (2) can be rewritten as

$$r(t) = \sqrt{\mathrm{x}}s(t) + \sum_{i=1}^{\mathrm{I}} \sqrt{\mathrm{y}_i}m_i(t) + \sum_{i=1}^{\mathrm{J}} \sqrt{\mathrm{z}_i}c_i(t) + w(t) \tag{3}$$

for the whole duration of the test packet, $1 \le t \le L$. Therefore, we can study the packet capture using the statistics of the snapshot of one symbol period.

2) Asynchronous Cochannel Cells: When inter-cell synchronization is not available (either by design or due to synchronization errors), the number of CCI packets may change within the transmission duration of the test packets and thus $\mathrm{J}(t)$ and $\mathrm{z}_i(t)$ can no longer be treated as constants. Referring to Fig. 2(b), the transmission interval of the test packet crosses the slot border of each cochannel cell and interferes to the packets transmitted in two consecutive slots. In other words, the number of CCI packets from one cochannel cell changes once in the transmission duration of the test packet. In addition, the instances of the change of the number of CCI packets from the cochannel cells are distinct from one another because the probability of coincidence of two or more instances of change is zero under the condition of asynchronization. Therefore, if

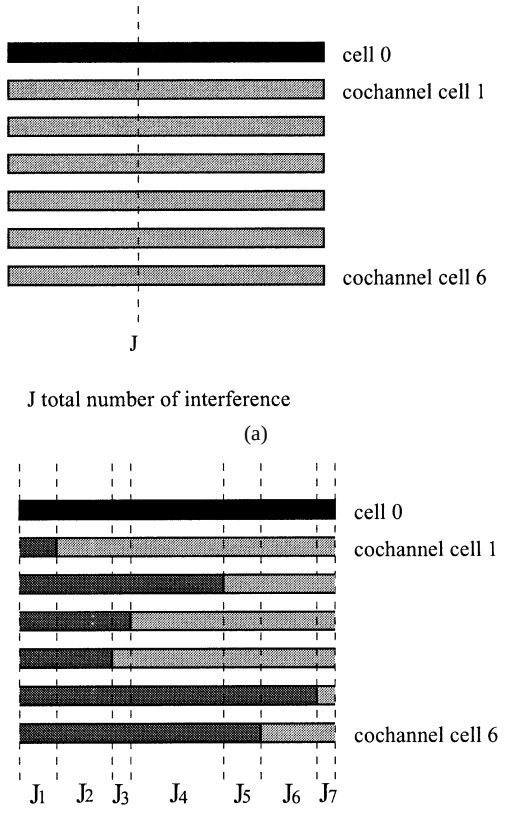

Fig. 2. Timing of (a) synchronized and (b) asynchronous CCI with the test packet (only the 6 first-tier cochannel cells are considered. The darkest shaded bar represents the test packet. The lighter shaded bars represents the packets of the 6 cochannel cells each, respectively. The two different shading of each bar in (b) mean two time slot in the corresponding cochannel cell in which different number of packets are under transmission).

N cochannel cells ($N = 6$ in Fig. 2(b) as a result that only the first-tier cochannel cells are considered and an omnidirectional antenna is used) are present, there will be N times of changes of the number of CCI packets in the transmission duration of the test packet, each caused by the change of one cochannel cell. The N times of changes results in $N + 1$ intervals of different CCI level for the test packet. Consequently, the received signal of (2) can be broken into $N + 1$ pieces with

$$r_n(t) = \sqrt{\mathrm{x}}s(t) + \sum_{i=1}^{\mathrm{I}} \sqrt{\mathrm{y}_i} m_i(t) + \sum_{i=1}^{\mathrm{J}_n} \sqrt{\mathrm{z}_{i,n}} c_{i,n}(t) + w(t) \quad (4)$$

representing the received signal in the nth interval, $1 \le n \le N + 1$, where J_n, $\mathrm{z}_{i,n}$ and $c_{i,n}(t)$ are correspondingly the number of CCI packets, the power of the tth symbol of the ith CCI packet associated with the nth interval. Note that J_n and $\mathrm{z}_{i,n}$ are short-term constant within the interval. We see that the signal capture condition is different from interval to interval. The packet capture happens when the test packet captures in each of the $N+1$ transmission intervals.

B. Nakagami Fading Channel

To characterize the statistical feature of the signal power x, y_is and z_is (or $\mathrm{z}_{i,n}$s for the case of asynchronous cochannel cells), a channel fading model is needed. In this paper, we adopt the Nakagami fading model [20]. This means that x, y_i and z_i $(\mathrm{z}_{i,n})$ are Γ-distributed random variables [26]. We further assume that all the MAI packets are with the same fading parameters and so are all the CCI packets. Suppose that the Nakagami fading parameters (amount of fading and mean power) for the test packet are $1/m_x$ and Ω_x, for the MAI packets are identically $1/m_y$ and Ω_y and for the CCI packets are identically $1/m_z$ and Ω_z. We require m_x, m_y and $m_z \ge 1/2$ and Ω_x, Ω_y and $\Omega_z > 0$. Then, the density functions of x, y_i and z_i are found to be [26]

$$f_{\mathrm{x}}(\xi) = \left(\frac{m_x}{\Omega_x}\right)^{m_x} \frac{\xi^{m_x-1}}{\Gamma(m_x)} \exp\left(-\frac{m_x}{\Omega_x}\xi\right) \quad (5)$$

$$f_{\mathrm{y}}(\xi) = \left(\frac{m_y}{\Omega_y}\right)^{m_y} \frac{\xi^{m_y-1}}{\Gamma(m_y)} \exp\left(-\frac{m_y}{\Omega_y}\xi\right) \quad (6)$$

$$f_{\mathrm{z}}(\xi) = \left(\frac{m_z}{\Omega_z}\right)^{m_z} \frac{\xi^{m_z-1}}{\Gamma(m_z)} \exp\left(-\frac{m_z}{\Omega_z}\xi\right) \quad (7)$$

respectively, where $\Gamma(\cdot)$ is the standard Gamma function. Note that when $m_x = 1$ (respective $m_y = 1$ or $m_z = 1$), (5) ((6) or (7)) degenerates to the exponential density function which corresponds to the Rayleigh fading case, i.e., Rayleigh fading is a special case of the Nakagami fading. Therefore, our analysis based on Nakagami model gives more general results.

III. Capture Effect Analysis

It is clear from (1) that the capture probability P_{cap} is the key point of the throughput analysis. In this section we first analyze the conditional capture probability for given numbers of MAI and CCI packets. We begin with the case of synchronized cochannel cells.

A. Synchronized Cochannel Cells

The test packet captures the receiver if its power supersedes that of the interference plus noise by a margin known as capture ratio η. In the case of synchronized cochannel cells, the packet capture is the same as the symbol capture. Therefore, according to (3), the probability of capture given I MAI and J CCI packets is

$$P_{\mathrm{cap}}(\mathrm{I}, \mathrm{J}) = \Pr\left\{\frac{\mathrm{x}}{\sum_{i=1}^{\mathrm{I}} \mathrm{y}_i + \sum_{i=1}^{\mathrm{J}} \mathrm{z}_i + W} \ge \eta\right\} \quad (8)$$

where W is the power of the additive noise.

Since y_is are mutually independent and identically Γ-distributed random variables as we have assumed in the previous section, the total MAI power $\mathrm{Y} = \sum_{i=1}^{\mathrm{I}} \mathrm{y}_i$ has the density function

$$f_{\mathrm{Y}}(\xi) = \left(\frac{m_y}{\Omega_y}\right)^{\mathrm{I}m_y} \frac{\xi^{\mathrm{I}m_y-1}}{\Gamma(\mathrm{I}m_y)} \exp\left(-\frac{m_y}{\Omega_y}\xi\right) \quad (9)$$

which can be easily derived from (6) using Laplace-Stieljes transform. Similarly, we can obtain the density function of the total CCI power $\mathrm{Z} = \sum_{i=1}^{\mathrm{J}} \mathrm{z}_i$ as

$$f_{\mathrm{Z}}(\xi) = \left(\frac{m_z}{\Omega_z}\right)^{\mathrm{J}m_z} \frac{\xi^{\mathrm{J}m_z-1}}{\Gamma(\mathrm{J}m_z)} \exp\left(-\frac{m_z}{\Omega_z}\xi\right). \tag{10}$$

$$\begin{aligned} f_{\mathrm{r}}(\xi|\mathrm{I},\mathrm{J}) &= \int_0^\infty \int_0^\infty (\alpha+\beta+W) f_{\mathrm{x}}(\xi(\alpha+\beta+W)) \\ &\quad \times f_{\mathrm{Y}}(\alpha) f_{\mathrm{Z}}(\beta) d\alpha d\beta \\ &= \frac{\left(\frac{m_x}{\Omega_x}\right)^{m_x}\left(\frac{m_y}{\Omega_y}\right)^{\mathrm{I}m_y}\left(\frac{m_z}{\Omega_z}\right)^{\mathrm{J}m_z}}{\Gamma(m_x)\Gamma(\mathrm{I}m_y)\Gamma(\mathrm{J}m_x)} \\ &\quad \times \xi^{m_x-1}\exp\left(-\frac{m_x}{\Omega_x}W\xi\right) \\ &\quad \cdot \int_0^\infty \int_0^\infty (\alpha+\beta+W)^{m_x}\alpha^{\mathrm{I}m_y-1}\beta^{\mathrm{J}m_z-1} \\ &\quad \times \exp\left[-\left(\frac{m_x}{\Omega_x}\xi+\frac{m_y}{\Omega_y}\right)\alpha\right] \\ &\quad \cdot \exp\left[-\left(\frac{m_x}{\Omega_x}\xi+\frac{m_z}{\Omega_z}\right)\beta\right] d\alpha d\beta \\ &= \frac{\left(\frac{m_x}{\Omega_x}\right)^{m_x}\left(\frac{m_y}{\Omega_y}\right)^{\mathrm{I}m_y}\left(\frac{m_z}{\Omega_z}\right)^{\mathrm{J}m_z}}{\Gamma(m_x)\Gamma(\mathrm{I}m_y)\Gamma(\mathrm{J}m_x)} \\ &\quad \times \xi^{m_x-1}\exp\left(-\frac{m_x}{\Omega_x}W\xi\right) \\ &\quad \cdot \sum_{k=0}^{m_x}\sum_{l=0}^{m_x-k} \frac{m_x!}{k!l!(m_x-k-l)!} W^{m_x-k-l} \\ &\quad \times \frac{\Gamma(\mathrm{I}m_y+k)\Gamma(\mathrm{J}m_z+l)}{\left(\frac{m_x}{\Omega_x}\xi+\frac{m_y}{\Omega_y}\right)^{\mathrm{I}m_y+k}\left(\frac{m_x}{\Omega_x}\xi+\frac{m_z}{\Omega_z}\right)^{\mathrm{J}m_z+l}} \\ &= \xi^{m_x-1}\exp\left(-\frac{m_x}{\Omega_x}W\xi\right) \\ &\quad \times \sum_{k=0}^{m_x}\sum_{l=0}^{m_x-k} \frac{m_x^{m_x-k-l+1}}{k!l!(m_x-k-l)!}\left(\frac{W}{\Omega_x}\right)^{m_x-k-l} \\ &\quad \cdot \frac{\Gamma(\mathrm{I}m_y+k)}{\Gamma(\mathrm{I}m_y)}\frac{\Gamma(\mathrm{J}m_z+l)}{\Gamma(\mathrm{J}m_z)} \frac{\left(\frac{m_x}{m_y}\frac{\Omega_y}{\Omega_x}\right)^k}{\left(\frac{m_x}{m_y}\frac{\Omega_y}{\Omega_x}\xi+1\right)^{\mathrm{I}m_y+k}} \\ &\quad \times \frac{\left(\frac{m_x}{m_z}\frac{\Omega_z}{\Omega_x}\right)^l}{\left(\frac{m_x}{m_z}\frac{\Omega_z}{\Omega_x}\xi+1\right)^{\mathrm{J}m_z+l}} \end{aligned} \tag{11}$$

Define the signal-to-interference-and-noise ratio (SINR) $\mathrm{r} = \mathrm{x}/(\mathrm{Y}+\mathrm{Z}+\mathrm{W})$. We derive the density function of r, $f_{\mathrm{r}}(\xi|\mathrm{I},\mathrm{J})$, as shown in (11). The third equality and after in (11) is valid for integer m_x. The fourth equality gives a more compacted version of the expression where the fading parameters of MAI and CCI are normalized with those of the test packet's.

Finally, the conditional capture probability $P_{\mathrm{cap}}(\mathrm{I},\mathrm{J})$ in (8) can be easily computed as

$$P_{\mathrm{cap}}(\mathrm{I},\mathrm{J}) = \int_\eta^\infty f_{\mathrm{r}}(\xi|\mathrm{I},\mathrm{J})d\xi. \tag{12}$$

B. Asynchronous Cochannel Cells

For the case of asynchronous cochannel cells, the packet capture probability can not be computed just based on received power of one symbol snapshot. Instead, we need to consider the SINR in each of the $N+1$ intervals (cf., (4)). For it to capture the receiver, the test packet must supersedes the interference in power by the capture ratio η in every interval. According to (4), the capture probability can be written as

$$\begin{aligned} &P_{\mathrm{cap}}(\mathrm{I},\mathrm{J}_1,\ldots,\mathrm{J}_{N+1}) \\ &\quad = \Pr\left\{\frac{\mathrm{x}}{\sum_{i=1}^{\mathrm{I}}\mathrm{y}_i + \sum_{i=1}^{\mathrm{J}_n}\mathrm{z}_{i,n}+W} \ge \eta, \right. \\ &\qquad \left. \text{for } n=1,\ldots,N+1\right\} \\ &\quad = \Pr\left\{\frac{\mathrm{x}}{\mathrm{Y}+\mathrm{Z}_n+W} \ge \eta, \quad \text{for } n=1,\ldots,N+1\right\} \end{aligned} \tag{13}$$

with obvious definitions for Y and Z_n's. It suffices that the capture condition is fulfilled in the interval with the maximum CCI power, i.e.,

$$P_{\mathrm{cap}}(\mathrm{I},\mathrm{J}_1,\ldots,\mathrm{J}_{N+1}) = \Pr\left\{\frac{\mathrm{x}}{\mathrm{Y}+\bar{\mathrm{Z}}+W} \ge \eta\right\} \tag{14}$$

where $\bar{\mathrm{Z}} = \max_{1\le n\le N+1}\mathrm{Z}_n$.

Deriving the distribution of $\bar{\mathrm{Z}}$ is nontrivial because Z_n's are correlated. We make the approximation that the interval of the maximum CCI power coincides that of the maximum number of CCI packets

$$\bar{\mathrm{Z}} \approx \sum_{i=1}^{\mathrm{J}_{\bar{n}}} z_{i,\bar{n}} \tag{15}$$

where $\bar{n}$ is such that $\mathrm{J}_{\bar{n}} = \max_{1\le n\le N+1}\mathrm{J}_n$. This approximation is reasonable considering that the CCI packets are assumed to be faded identically (also independently) and there are large number of them from each of the six cochannel cells. It will also be justified using simulations in later sections. Denote $\mathrm{J}_{\bar{n}}$ with $\bar{\mathrm{J}}$. It is easy to obtain the density function of $\bar{\mathrm{Z}}$, as

$$f_{\bar{\mathrm{Z}}}(\xi) = \left(\frac{m_z}{\Omega_z}\right)^{\bar{\mathrm{J}}} m_z \frac{\xi^{\bar{\mathrm{J}}m_z-1}}{\Gamma(\bar{\mathrm{J}}m_z)}\exp\left(-\frac{m_z}{\Omega_z}\xi\right). \tag{16}$$

Then we can follow similar procedures of (11) to get the density function of the SINR in the maximum CCI power interval $\bar{\mathrm{r}} = \mathrm{x}/(\mathrm{Y}+\bar{\mathrm{Z}}+W)$ as

$$\begin{aligned} &f_{\bar{\mathrm{r}}}(\xi|\mathrm{I},\mathrm{J}_1,\ldots,\mathrm{J}_{N+1}) \\ &\quad = \xi^{m_x-1}\exp\left(-\frac{m_x}{\Omega_x}W\xi\right)\sum_{k=0}^{m_x}\sum_{l=0}^{m_x-k}\frac{m_x^{m_x-k-l+1}}{k!l!(m_x-k-l)!} \\ &\qquad \cdot \left(\frac{W}{\Omega_x}\right)^{m_x-k-l}\frac{\Gamma(\mathrm{I}m_y+k)}{\Gamma(\mathrm{I}m_y)}\frac{\Gamma(\bar{\mathrm{J}}m_z+l)}{\Gamma(\bar{\mathrm{J}}m_z)} \\ &\qquad \cdot \frac{\left(\frac{m_x}{m_y}\frac{\Omega_y}{\Omega_x}\right)^k}{\left(\frac{m_x}{m_y}\frac{\Omega_y}{\Omega_x}\xi+1\right)^{\mathrm{I}m_y+k}}\frac{\left(\frac{m_x}{m_z}\frac{\Omega_z}{\Omega_x}\right)^l}{\left(\frac{m_x}{m_z}\frac{\Omega_z}{\Omega_x}\xi+1\right)^{\bar{\mathrm{J}}m_z+l}} \end{aligned} \tag{17}$$

only replacing J in (11) with $\bar{\mathrm{J}}$. The conditional capture probability follows straightforwardly as

$$P_{\mathrm{cap}}(\mathrm{I},\mathrm{J}_1,\ldots,\mathrm{J}_{N+1})=\int_{\eta}^{\infty} f_{\bar{\mathrm{r}}}(\xi|\mathrm{I},\mathrm{J}_1,\ldots,\mathrm{J}_{N+1})d\xi. \quad (18)$$

C. Consideration of Shadowing

The previous sections have focused on the channel fading effects on the capture probability. The additive noise has also been taken care of in the expression, so the minimum transmission power constraint has been embedded. What is yet to be addressed is the shadowing effect caused by buildings, hills and trees obstructing the radio signal. The shadowing effect results in random variations in the signal mean power Ω_x, Ω_y and Ω_z. The randomness is usually modeled with the lognormal distribution, e.g.,

$$f_{\Omega_x}(\xi)=\frac{C_x}{\xi}\exp\left[-\frac{(\log\xi+A_x)^2}{B_x}\right],\quad \xi>0 \quad (19)$$

where

$$C_x=\frac{\log e}{\sqrt{2\pi}\sigma_x}$$
$$A_x=-\log\Omega_{0x}+\frac{\sigma_x^2}{2\log e},$$
$$B_x=2\sigma_x^2$$

and Ω_{0x} is the mean value of Ω_x and σ_x is the standard deviation in bels. Similar density functions for Ω_y and Ω_z exist.

To take into account the random variations in Ω_x, Ω_y and Ω_z in the capture probability, we can view (11) or (17) as conditioned on the signal mean powers, Ω_x, Ω_y and Ω_z, and average them statistically. The results are

$$f_{\mathrm{r}}(\xi|\mathrm{I},\mathrm{J})=\int_0^{\infty}\int_0^{\infty}\int_0^{\infty}\frac{\left(\frac{m_x}{\xi_1}\right)^{m_x}\left(\frac{m_y}{\xi_2}\right)^{\mathrm{I}m_y}\left(\frac{m_z}{\xi_3}\right)^{\mathrm{J}m_z}}{\Gamma(m_x)\Gamma(\mathrm{I}m_y)\Gamma(\mathrm{J}m_x)}$$
$$\cdot\xi^{m_x-1}\exp\left(-\frac{m_x}{\xi_1}W\xi\right)\sum_{k=0}^{m_x}\sum_{l=0}^{m_x-k}\frac{m_x!}{k!l!(m_x-k-l)!}$$
$$\cdot W^{m_x-k-l}\frac{\Gamma(\mathrm{I}m_y+k)\Gamma(\mathrm{J}m_z+l)}{\left(\frac{m_x}{\xi_1}\xi+\frac{m_y}{\xi_2}\right)^{\mathrm{I}m_y+k}\left(\frac{m_x}{\xi_1}\xi+\frac{m_z}{\xi_3}\right)^{\mathrm{J}m_z+l}}$$
$$\times f_{\Omega_x}(\xi_1)f_{\Omega_y}(\xi_2)f_{\Omega_z}(\xi_3)d\xi_1d\xi_2d\xi_3 \quad (20)$$

for the case of synchronized cochannel cells and

$$f_{\bar{\mathrm{r}}}(\xi)=\int_0^{\infty}\int_0^{\infty}\int_0^{\infty}\frac{\left(\frac{m_x}{\xi_1}\right)^{m_x}\left(\frac{m_y}{\xi_2}\right)^{\mathrm{I}m_y}\left(\frac{m_z}{\xi_3}\right)^{\bar{\mathrm{J}}m_z}}{\Gamma(m_x)\Gamma(\mathrm{I}m_y)\Gamma(\bar{\mathrm{J}}m_x)}$$
$$\cdot\xi^{m_x-1}\exp\left(-\frac{m_x}{\xi_1}W\xi\right)\cdot\sum_{k=0}^{m_x}\sum_{l=0}^{m_x-k}\frac{m_x!}{k!l!(m_x-k-l)!}$$
$$\cdot W^{m_x-k-l}\frac{\Gamma(\mathrm{I}m_y+k)\Gamma(\bar{\mathrm{J}}m_z+l)}{\left(\frac{m_x}{\xi_1}\xi+\frac{m_y}{\xi_2}\right)^{\mathrm{I}m_y+k}\left(\frac{m_x}{\xi_1}\xi+\frac{m_z}{\xi_3}\right)^{\bar{\mathrm{J}}m_z+l}}$$
$$\times f_{\Omega_x}(\xi_1)f_{\Omega_y}(\xi_2)f_{\Omega_z}(\xi_3)d\xi_1d\xi_2d\xi_3. \quad (21)$$

for the case of asynchronous cochannel cells. Finally, the capture probability can be computed using (12) and (18).

IV. Packet Throughput

After obtaining the capture probability for given number of MAI and CCI packets, $P_{\mathrm{cap}}(\mathrm{I},\mathrm{J})$ or $P_{\mathrm{cap}}(\mathrm{I},\mathrm{J}_1,\ldots,\mathrm{J}_{N+1})$, we can get the average capture probability as

$$P_{\mathrm{cap}}=\sum_{i=0}^{\infty}\sum_{j=0}^{\infty}P_{\mathrm{cap}}(i,j)P(\mathrm{I}=i)P(\mathrm{J}=j) \quad (22)$$

for the case of synchronized cochannel cells and

$$P_{\mathrm{cap}}=\sum_{i=0}^{\infty}\sum_{j_1,\ldots,j_{N+1}=0}^{\infty}P_{\mathrm{cap}}(i,j_1,\ldots,j_{N+1})P(\mathrm{I}=i)$$
$$\cdot P(\mathrm{J}_1=j_1,\ldots,\mathrm{J}_{N+1}=j_{N+1}) \quad (23)$$

for the case of asynchronous cochannel cells, where the mass functions $P(\mathrm{I}=i)$, $P(\mathrm{J}=j)$ and $P(\mathrm{J}_1=j_1,\ldots,\mathrm{J}_{N+1}=j_{N+1})$ is determined by the traffic characteristics. In this section, we are to derive the mass functions of I and J. Again, we start with the case of synchronized cochannel cells.

A. Synchronous Cochannel Cells

The distribution of the number of MAI and CCI packets, I and J are quite straightforward under the assumption of Poisson arrivals with rate G per channel slot per cell. It is easy to obtained that

$$P(\mathrm{I}=i)=\frac{G^i}{i!}\exp(-G) \quad (24)$$
$$P(\mathrm{J}=j)=\frac{(NG)^j}{j!}\exp(-NG) \quad (25)$$

In (25), N is the number the cochannel cells. When only the first-tier cochannel cells are considered and an omnidirectional antenna is used, $N=6$.

B. Asynchronous Cochannel Cells

In the case of asynchronous cells, we need to evaluate the joint distribution of $\mathrm{J}_1,\ldots,\mathrm{J}_{N+1}$. That is not an easy task because J_n's are correlated. However, the conditional capture probability $P_{\mathrm{cap}}(\mathrm{I},\mathrm{J}_1,\ldots,\mathrm{J}_{N+1})=P_{\mathrm{cap}}(\mathrm{I},\bar{\mathrm{J}})$ depends on $\bar{\mathrm{J}}$, the maximum one among J_ns according to (17). So we can study the distribution of $\bar{\mathrm{J}}$ instead. Direct evaluation of the distribution of $\bar{\mathrm{J}}$ still needs the joint statistics of J_ns. But we note that the interference from each cochannel cells are divided into two epochs within the considered duration of the transmission of the test packet (see Fig. 2(b)). Let us denote the number of the interfering packets in the two epochs with $\mathrm{J}^{k,1}$ and $\mathrm{J}^{k,2}$ for the kth cochannel cell, $k=1,\ldots N$. Let us additionally define $\mathrm{J}^k=\max\{\mathrm{J}^{k,1},\mathrm{J}^{k,2}\}$. Then, the sum of J^ks is an upper bound of $\bar{\mathrm{J}}$,

$$\bar{\mathrm{J}}\le\tilde{\mathrm{J}}=\sum_{k=1}^{N}\max\{\mathrm{J}^{k,1},\mathrm{J}^{k,2}\} \quad (26)$$

and we will use $\tilde{\mathrm{J}}$ in place of $\bar{\mathrm{J}}$. Using the upper bound $\tilde{\mathrm{J}}$ will result in a lower bound of the throughput value. It turns out, according to our simulations in later sections, that this is so tight a bound that it almost coincides the real throughput.

Since $\mathrm{J}^{k,l}$, $k = 1,\ldots,N$, $l = 1, 2$ are independent and identically distributed Poisson variables of G, the derivation of the distribution of $\tilde{\mathrm{J}}$ is easy. We have

$$P(\mathrm{J}^{k,l} = j) = \frac{G^j}{j!}e^{-G},\ k = 1,\ldots,N, l = 1, 2. \tag{27}$$

Based on it, it is easy to obtain that

$$\begin{aligned} P(\mathrm{J}^k = j) &= \Pr\{\mathrm{J}^{k,1} = j, \mathrm{J}^{k,2} \le j\} + Pr\{\mathrm{J}^{k,1} \le j, \mathrm{J}^{k,2} = j\} \\ &\quad - \Pr\{\mathrm{J}^{k,1} = J^{k,2} = j\} \\ &= \left(2\sum_{m=0}^{j}\frac{G^m}{m!} - \frac{G^j}{j!}\right)\frac{G^j}{j!}e^{-2G} \\ &= \left(2\sum_{m=0}^{j-1}\frac{G^m}{m!} + \frac{G^j}{j!}\right)\frac{G^j}{j!}e^{-2G} \\ &\quad k = 1,\ldots,N. \end{aligned} \tag{28}$$

In addition, J^ks are independent. $\tilde{\mathrm{J}}$ is the sum of the independent and identically distributed random variables J^k, $k = 1,\ldots,N$. Therefore, its mass function can be expressed as

$$\begin{aligned} P(\tilde{\mathrm{J}} = j) &= P(\mathrm{J}^1 = j) \otimes P(\mathrm{J}^2 = j) \ldots \otimes P(\mathrm{J}^N = j) \\ &= \sum_{j_1+\ldots+j_N=j}\prod_{k=1}^{N} P(\mathrm{J}^k = j_k) \end{aligned} \tag{29}$$

where $\otimes$ represents convolution sum. Since $N = 6$, evaluation of (29) will not be difficult.

With the expressions of the distributions of I and J, (24) and (25) [or (29)], as well as the conditional capture probability (12) [or (18)] obtained in the previous sections, we can compute the packet capture probability according to (22); and the result can be used to evaluate the system throughput.

V. Effect of Cluster Size

In this section, we relate the cluster size of a cellular systems to the system throughput. First, we need to modify the definition of throughput in (1) in order to make fair comparisons among the throughput performance of different cluster sizes. For a given coverage, the number of clusters needed is inversely proportional to the cluster size. Since one channel is reused the same times as the number of clusters, the throughput per unit coverage area should be that defined in (1) divided by the cluster size. Therefore, for a cluster of C cells, we shall use S/C as the measure of the system throughput.

We consider the cellular system with omni-cells having fixed size and geographically uniform traffic. The cluster size C of a cellular system is related to the cochannel reuse distance U as (e.g., [28])

$$U = \sqrt{3C} \tag{30}$$

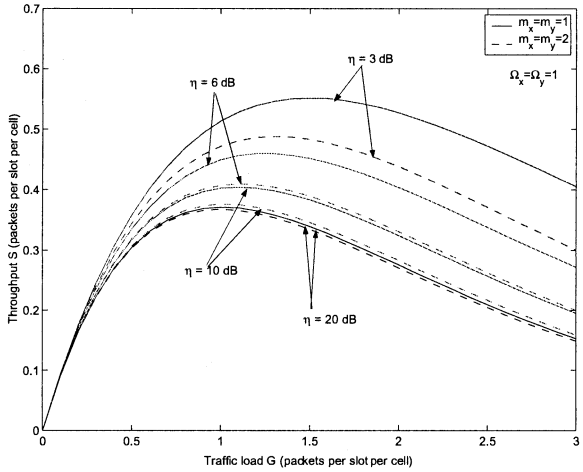

Fig. 3. MAI only and no CCI: The same fading parameters are used for the test packet and the MAI packets; the average power is set to $\Omega_x = \Omega_y = 1$; two fading amount parameters, $m_x = m_y = 1$ (Rayleigh fading) and 2 are set; four capture margins $\eta = 3$, 6, 10, 20 dB are computed; the computation is performed by setting $\Omega_z = 0$ in (11).

where U is defined as the ratio of distance between the centers of nearest neighboring cochannel cells D and the cell radius R, i.e.,

$$U = \frac{D}{R}. \tag{31}$$

According to the path loss model, the ratio between the mean power of the considered packet and of the CCI is

$$\frac{\Omega_x}{\Omega_z} = \left(\frac{D}{R}\right)^{\gamma} = U^{\gamma} \tag{32}$$

where $2 \le \gamma \le 6$ is the attenuation rate. Substituting (30) and (32) into (11) (or (17)), we can easily obtain the capture probability as a function of the cluster size. The distribution of the number of MAI and CCI packets in both synchronized and asynchronous cochannel cell cases for given traffic load G can be borrowed from previous section with no changes. The relation of the system throughput and the cluster size thus follows.

VI. Numerical Results

This section provides some plots to visualize the expressions derived in the previous sections. All the plots show the throughput S versus the traffic load G. Simulations results are also provided in parallel with the numerical plots when necessary to justify the theoretic analysis. The simulation was performed for a duration equivalent to 100 000 time slots. Since we mainly focus on the interference issue, noise has been omitted in the theoretical computations and simulations, i.e., $W = 0$, even though both can incorporate the noise effect easily.

We first give the plots for the case of MAI only with no CCI, $\Omega_z = 0$. This is the case having been addressed in past studies. It is included however, for completeness and verification. Results for two sets of fading parameters as annotated on the plots are shown in Fig. 3. Those results are consistent with other researchers' work, e.g., [14], [24] implying that our result is more general and can degenerate to simpler cases studied previously.

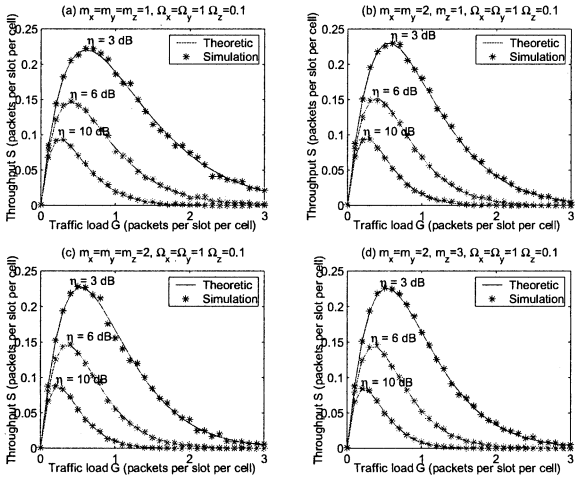

Fig. 4. MAI and synchronized CCI. Four sets of fading parameters as shown in the title of each subfigure are computed; the average power of the CCI packets are set to be 10 dB below the test packet and the MAI packets $\Omega_x/\Omega_z = 10$; three capture margins are computed; the theoretic results are obtained through numerical evaluation of (12), (24), (25), and (22) and simulation results are obtained by Monte Carlo simulation of (3) and (8).

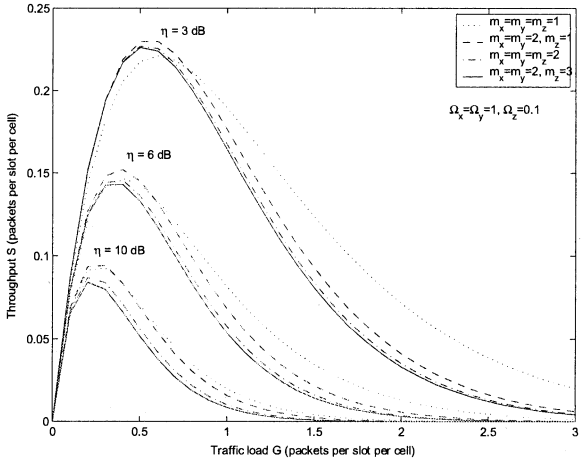

Fig. 5. MAI and synchronized CCI. Comparison among different sets of fading parameters are made by reproducing the theoretic results from four subfigures of Fig. 4.

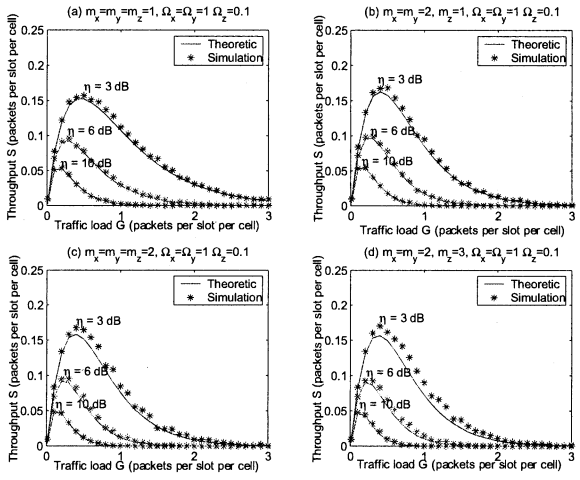

Fig. 6. MAI and asynchronous CCI. The same fading parameter setup as Fig. 4 are used except CCI packets are asynchronous; the theoretic results are obtained through numerical evaluation of (18), (24), (29), and (22) and simulation results are obtained by Monte Carlo simulation of (4) and (13).

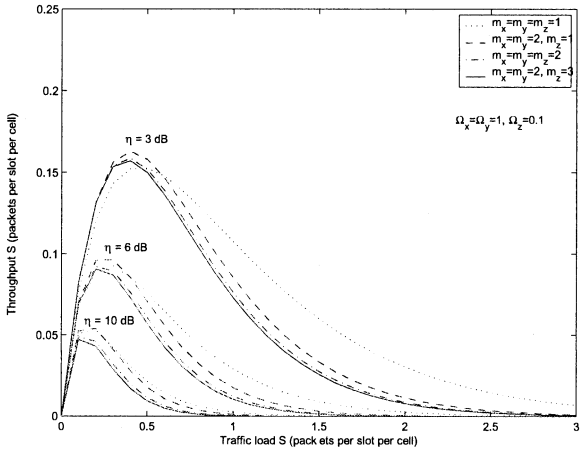

Fig. 7. MAI and asynchronous CCI: Comparison among different sets of fading parameters are made by reproducing the theoretic results from four subfigures of Fig. 6.

Note that the curve corresponding to $\eta = 20\ dB$ is practically the throughput for standard S-ALOHA.

The second group of results show the effect of CCI in addition to that of MAI. Fig. 4 is for the case of synchronized cochannel cells and Fig. 6 asynchronous. Results of four sets of fading parameters are shown. Simulation results are shown against the theoretic results. For comparison purposes, the theoretic data for the four sets of fading parameters are reproduced in Fig. 5 and 7, respectively, from which we see that the existence of CCI significantly degrades the throughput performance, and that the more the amount of fading of the interference, the more the throughput reductions. Fig. 8 is also a reproduction of the data from Fig. 4 and 6, which compares the synchronized and asynchronous cochannel cell cases for a chosen set of parameters, $m_x = m_y = 2, m_z = 1, \Omega_x = \Omega_y = 1, \Omega_z = 0.1$. It can be seen that asynchronism causes much more serious throughput reduction. This is because that asynchronism causes fluctuation of the interference, which lowers the capture probability. Conceptually speaking, the packet capture for the asynchronous case is only possible when the capture margin is exceeded in all the $N + 1$ intervals of different CCI level [cf. Fig. 2 and (13)]. If we perceive that the capture effect in each interval are independent and the capture probability in each interval is the same and equal to the packet capture probability of the synchronized case, say p, the packet capture probability for the asynchronous case would be only p^N, which can be significantly lower than p when p is small. Though the correlation among the number of CCI packets in succeeding intervals may somehow limit the extent of this trend, it does not completely offset it.

Another issue deserving special notice is that the highly consistency of the simulation and theoretic results, especially in the asynchronous case where approximations have been made for

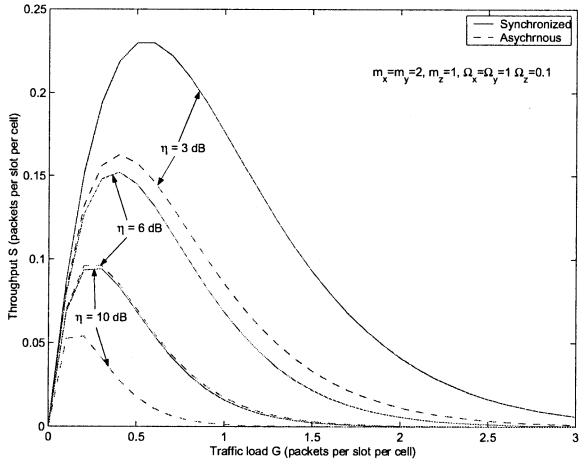

Fig. 8. Comparison for synchronized and asynchronous cases for the fading parameter set, $m_x = m_y = 2, m_z = 1, \Omega_x = \Omega_y = 1, \Omega_z = 0.1$; the plots are reproduced from the corresponding ones in Fig. 4 and 6.

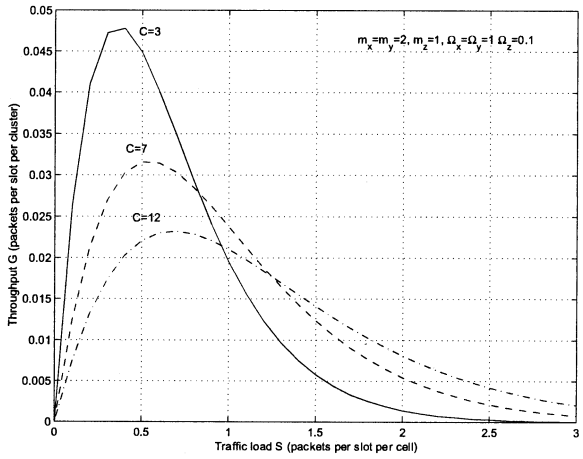

Fig. 10. Effects of cluster size for synchronized CCI case under the fading parameters. $m_x = m_y = 2, m_z = 1, \Omega_x = \Omega_y = 1, \omega_z = 0.1$.

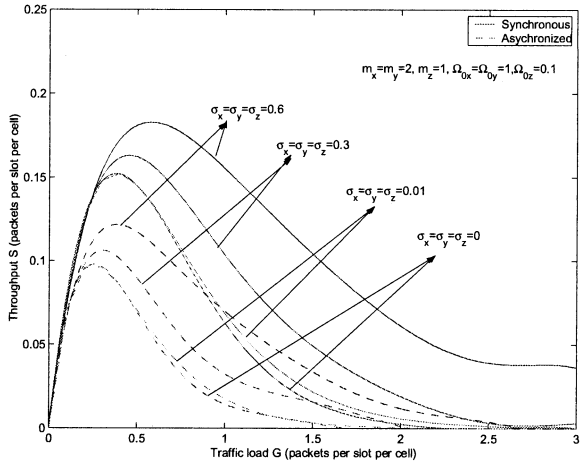

Fig. 9. Fading and lognormal shadowing: $m_x = m_y = 2, m_z = 1, \Omega_{0x} = \Omega_{0y} = 1, \omega_{0z} = 0.1, \sigma_x = \sigma_y = \sigma = 0.01/0.3/0.6$; the results are obtained through numerical evaluation of (20)/(21), (12)/(18), (24), (25) and (22); the curves of $\sigma_x = \sigma_y = \sigma_z = 0$ are reproduction of the middle curves $(\eta = 6\ \mathrm{dB})$ in Fig. 4(b) and (6b).

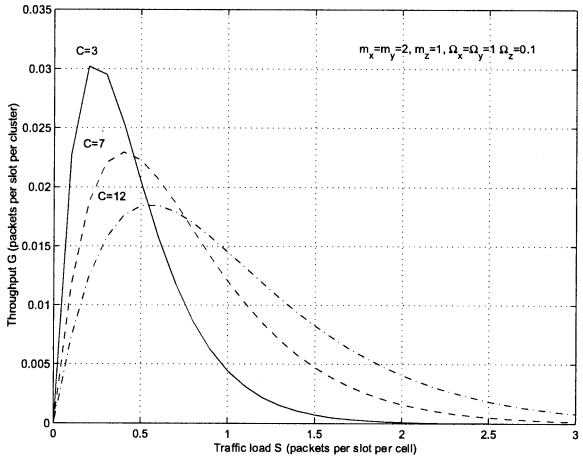

Fig. 11. Effects of cluster size for asynchronous CCI under the fading parameters. $m_x = m_y = 2, m_z = 1, \Omega_x = \Omega_y = 1, \omega_z = 0.1$.

mathematical tractability (cf. Section III-B and IV-B). The simulation results are obtained by Monte Carlo simulation of (3) and (8).

The shadowing, in addition to fading, is considered in plotting Fig. 9 for both synchronous and asynchonized CCI cases. The fading parameters are $m_x = m_y = 2, m_z = 1, \Omega_{0x} = \Omega_{0y} = 1, \Omega_{0z} = 0.1$, and $\sigma_x = \sigma_y = \sigma_z = 0.01/0.3/0.6$ bel. The capture margin η is 6 dB. The results are compared those in Fig. 4(b) and (6b) with corresponding parameters. Actually, the curves of $\sigma_x = \sigma_y = \sigma_z = 0$ are reproduction of middle curves $(\eta = 6\ \mathrm{dB})$ in Fig. 4(b) and (6b). We observe that shadowing benefits the throughput and the more the variation of the average power the higher the throughput. This is of course because that shadowing causes more variations of the received signal power and enhances the capture effect.

The throughput performance for different cluster sizes of the cellular system is shown in Fig. 10 and 11 for the synchronized and asynchronous CCI cases, respectively. Note that the y-coordinate here is S/C instead of S. We see that under light to moderate traffic load, systems of small cluster size offer better performance. This is because the higher frequency reuse ratio. Under heavy traffic conditions however, large cluster size outperforms. A qualitative explanation is that in heavy traffic, CCI causes significant reduction of the throughput per cell that outweighs the spatial reuse factor.

VII. Conclusion

We have developed a theoretic framework for the throughput analysis of S-ALOHA in a cellular system and Nakagami fading environment. Our paper is consistent with previous results on the effects of MAI and signal capture to the throughput of S-ALOHA. We additionally included in our analysis the CCI which is an important issue when multicell scenarios are considered; and our analyzes showed that CCI, especially in an asynchronous mode, has a significant impairment on the throughput performance. This may suggest that a proper

system-wide synchronization is necessary to achieve high system throughput.

Since many other system parameters and channel conditions can be easily incorporated, the developed framework can be used for system design and optimization. For example, since CCI is related to the channel reuse distance of a cellular system, the cluster size comes into the expression of the throughput and its effect is not so obvious. Though a smaller cluster size benefits the system throughput through higher frequency reuse rate, the benefit can be offset by the increased CCI level. Therefore, certain optimization is necessary. Other applications may include admission control to adjust the traffic rate to achieve the higher throughput.

REFERENCES

[1] N. Abramson, "The Aloha system—another alternative for computer communications," in *Proc. Fall Joint Comput. Conf. AFIPS Conf.*, 1970, p. 37.

[2] D. Bertsekas and R. Gallager, *Data Networks*, 2nd ed. Englewood Cliffs: Prentice-Hall, 1992.

[3] L. G. Roberts, "ALOHA packet systems with and without slot and capture," *Computer Communications Review*, vol. 51, pp. 28–42, April 1975.

[4] C. T. Lau and C. Leung, "Capture models for mobile packet radio networks," *IEEE Trans. Commun.*, vol. 40, pp. 917–925, May 1992.

[5] C. Fratta and D. Sant, "Some models of packet radio networks with capture," in *Proc. ICC*, 1980, pp. 155–161.

[6] K. Zhang and K. Pahlavan, "A new approach for the analysis of the slotted ALOHA local radio networks," in *Proc. ICC*, 1990, pp. 1231–1235.

[7] ——, "Relation between transmission and throughput of slotted ALOHA local packet radio networks," *IEEE Trans. Commun.*, vol. 40, pp. 577–583, Mar. 1992.

[8] J. A. Roberts and T. J. Healy, "Packet radio performance over slow Rayleigh fading channels," *IEEE Trans. Commun.*, vol. 28, pp. 279–286, Feb. 1980.

[9] F. Kuperus and J. Arnbak, "Packet radio in a Rayleigh channel," *Elec. Lett.*, vol. 18, no. 12, pp. 506–507, 1982.

[10] J. C. Arnbak and W. V. Blitterswijk, "Capacity of slotted ALOHA in Rayleigh fading channels," *IEEE J. Sel. Areas Commun.*, vol. 5, pp. 261–269, 1987.

[11] E. Zainal and R. Garcia, "The effects of Rayleigh fading on capture phenomenon in ALOHA channels," in *Proc. INFOCOM*, 1987, pp. 888–893.

[12] R. Prasad and J. Arnbak, "Enhanced throughput in packet radio channels with fading and shadowing," in *Proc. Canadian Conf. Elec. Comput. Eng.*, 1988, pp. 78–80.

[13] A. Sheikh, Y. D. Yao, and X. Wu, "The ALOHA systems in shadowed mobile radio channels with slow or fast fading," *IEEE Trans. Veh. Technol.*, vol. 39, pp. 289–298, 1990.

[14] Y. D. Yao and A. U. H. Sheikh, "Outage probability analysis for microcell mobile radio systems with cochannel interferers in Rician/Rayleigh fading environment," *Electro. Lett.*, vol. 26, pp. 864–866, June 1990.

[15] C. van der Plas and J. P. Linnartz, "Stability of mobile slotted AlOHA network with Rayleight fading, shadowing and near-far effects," *IEEE Trans. Veh. Technol.*, vol. 39, pp. 359–366, 1990.

[16] J. P. Linnartz, "Near-far effects in land mobile random access networks with narrow-band Rayleigh fading channels," *IEEE Trans. Veh. Technol.*, vol. 41, pp. 77–89, Feb. 1992.

[17] ——, "Slotted ALOHA land-mobile radio networks with site diversity," *IEE Proc.-I*, vol. 139, pp. 58–70, Feb. 1992.

[18] K. Zhang and K. Phalavan, "Slotted ALOHA radio networks with PSK modulation in Rayleigh fading channels," *Electron. Lett.*, pp. 412–413, Mar. 1989.

[19] H. Yang and M. Alouini, "Throughput of slotted aloha systems in mixed Rician-Nakagami fading environments with a minimum signal power constraint," in *Proc. ICC*, vol. 6, 2001, pp. 1723–1727.

[20] M. Nakagami, "The m-distribution—a general formula of intensity distribution of rapid fading," in *Statistical Methods of Radio Wave Propagation*, W. Hoffman, Ed. New York: Pergamon, 1960, pp. 3–36.

[21] S. A. Al-Semari and M. Guizani, "Channel throughput of slotted ALOHA in a Nakagami fading environment," in *Proc. ICC*, June 1997, pp. 605–609.

[22] M. Abdel-Hafez and M. Safak, "Correlated shadowing and near-far effects on throughput of slotted ALOHA in Nakagami fading environment," in *Proc. 9th Mediterranean Electrotech. Conf.*, May 1998, pp. 721–725.

[23] ——, "Throughput of slotted ALOHA in Nakagami fading and correlated shadowing environment," *Electron. Lett.*, vol. 33, pp. 1024–1025, June 1997.

[24] S. A. Al-Semari and N. Grami, "A general expression for the capacity of slotted ALOHA under Nakagami fading," in *Proc. WCNC*, 1999, pp. 849–853.

[25] A. A. Abu-Dayya and N. C. Beaulieu, "Outage probabilities of cellular mobile radio systems with multiple Nakagami interferers," *IEEE Trans. Veh. Technol.*, vol. 40, pp. 757–768, Nov. 1991.

[26] Y. D. Yao and A. U. H. Sheikh, "Investigations into cochannel interference in microcellular mobile radio systems," *IEEE Trans. Veh. Technol.*, vol. 41, pp. 114–123, May 1992.

[27] Q. T. Zhang, "Outage probability in cellular mobile radio due to Nakagami signal and interferers with arbitrary parameters," *IEEE Trans. Veh. Technol.*, vol. 45, pp. 364–372, May 1996.

[28] V. K. Garg and J. E. Wilkes, *Wireless and Personal Communications Systems*. Englewood Cliffs, NJ: Prentice-Hall PTR, 1996.

Lei Zhou (S'99) received the B.S. degree in mechanical-electronic engineering and the M.E. degree in electrical engineering from Beijing Institute of Technology, Beijing China, in 1993 and 1997, respectively, and the M.S. degree in computer science from Stevens Institute of Technology, Hoboken, NJ, in 2000.

She is currently a Ph.D. degree candidate with the Electrical and Computer Engineering Department, Stevens Institute of Technology. She has been a graduate assistant with the Computer Science and Electrical and Computer Engineering Departments of Stevens Institute of Technology since 1998. Her research area is wireless networking with focus on packet radio, medium access, and CDMA.

Yu-Dong Yao (S'88–M'88–SM'94) received the B.Eng. and M.Eng. degrees from Nanjing University of Posts and Telecommunications, Nanjing, China, in 1982 and 1985, respectively, and the Ph.D. degree from Southeast University, Nanjing, in 1988, all in electrical engineering.

Between 1989 and 1990, he was with Carleton University, Ottawa, as a Research Associate working on mobile radio communications. He was with Spar Aerospace Ltd., Montreal, between 1990 and 1994, where he was involved in research on satellite communications. He was with Qualcomm Inc., San Diego, CA, from 1994 to 2000, where he participated in research and development in wireless CDMA systems. He joined Stevens Institute of Technology, Hoboken, NJ, in 2000. He is an Associate Professor with the Department of Electrical and Computer Engineering and a Director of Wireless Information Systems Engineering Laboratory (WISELAB). He holds one Chinese patent and seven U.S. patents. His research interests include wireless communications and networks, spread spectrum and CDMA, and DSP for wireless systems.

Dr. Yao is an Associate Editor of the IEEE COMMUNICATIONS LETTERS and the IEEE TRANSACTIONS ON VEHICULAR TECHNOLOGY, and an Editor of the IEEE TRANSACTIONS ON WIRELESS COMMUNICATIONS.

Harry Heffes (M'66–SM'82–F'90) received the B.E.E. degree from City College of New York, NY, in 1962, and the M.E.E. and Ph.D. degrees in electrical engineering from New York University, Bronx, NY, in 1964 and 1968, respectively.

He joined the Department of Electrical Engineering and Computer Science, Stevens Institute of Technology, Hoboken, NJ, in 1990. He assumed the faculty position of Professor of Electrical Engineering and Computer Science after a 28-year career with AT&T Bell Laboratories. In his early years at Bell Labs, he worked on the Apollo Lunar Landing Program, where he applied modern control and estimation theory to problems relating to guidance, navigation, tracking and trajectory optimization. More recently, his primary concern has been with the modeling, analysis, and overload control of telecommunication systems and services. He is the author of more than 25 papers in a broad range of areas including voice and data communication networks, overload control for distributed switching systems, queuing, and teletraffic theory and applications, as well as computer performance modeling and analysis.

Dr. Heffes received the Bell Labs Distinguished Technical Staff Award in 1983 and, for his work on modeling packetized voice traffic, he was awarded the IEEE Communication Society's S.O. Rice Prize in 1986. He is a Fellow the IEEE for his contributions to teletraffic theory and applications. He has served as a United States Delegate to the International Teletraffic Congress and as an Associate Editor for *NETWORKS: An International Journal*. He is a Member of Eta Kappa Nu, Tau Beta Pi, American Men and Women of Science, and is listed in *Who's Who in America*.

Ruifeng Zhang (S'97–M'00) received the B.S. degree from Huazhong University of Science and Technology, Wuhan, China, in 1993, the M.E. degree from Beijing Institute of Technology, Beijing, China, in 1996, and the Ph.D. degree from Stevens Institute of Technology, Hoboken, NJ, in 2000, all in electrical engineering.

He joined the Electrical and Computer Engineering Department, Drexel University, Philadelphia, PA, in 2000, where he is an Assistant Professor. He was a Research Assistant and Postdoctoral Associate with the Electrical and Computer Engineering Department, Stevens Institute of Technology, during 1997–2000. His general research interests lie in the areas of statistical signal processing and communications. The current focus of his work is on signal processing methods for wireless networks. He has authored and coauthored more than 40 technical papers in referred journals of conferences.

Dr. Zhang received the 2002 IEEE Signal Processing Society Best Paper Award for his paper entitled "Network assisted diversity multiple access for wireless data networks" (IEEE TRANSACTIONS ON SIGNAL PROCESSING, 2000). He is Chair of the joint SP/BT/CE Chapter, IEEE Philadelphia Section. He serves on the organizing committee for the 2005 ICASSP. He received the Peskin Award from Stevens Institute of Technology in 2000 and the AT&T and ACM Student Research Award in 1999.